Rigid cyclic fluorinated detergents: fine-tuning the hydrophilic–lipophilic balance controls self-assembling and biochemical properties

Marine Soulié, Anais Deletraz, Moheddine Wehbie, Florian Mahler, Benjamin Chantemargue, Ilham Bouchemal, Aline Le Roy, Isabelle Petit-Härtlein, Franck Fieschi, Cécile Breyton, et al.

▶ **To cite this version:**

Marine Soulié, Anais Deletraz, Moheddine Wehbie, Florian Mahler, Benjamin Chantemargue, et al.. Rigid cyclic fluorinated detergents: fine-tuning the hydrophilic–lipophilic balance controls self-assembling and biochemical properties. ACS Applied Materials & Interfaces, 2024, 16 (26), pp.32971-32982. 10.1021/acsami.4c03359 . hal-04637060

HAL Id: hal-04637060
https://hal.science/hal-04637060v1

Submitted on 5 Jul 2024

HAL is a multi-disciplinary open access archive for the deposit and dissemination of scientific research documents, whether they are published or not. The documents may come from teaching and research institutions in France or abroad, or from public or private research centers.

L'archive ouverte pluridisciplinaire **HAL**, est destinée au dépôt et à la diffusion de documents scientifiques de niveau recherche, publiés ou non, émanant des établissements d'enseignement et de recherche français ou étrangers, des laboratoires publics ou privés.

ACS APPLIED MATERIALS & INTERFACES

www.acsami.org Research Article

Rigid Cyclic Fluorinated Detergents: Fine-Tuning the Hydrophilic−Lipophilic Balance Controls Self-Assembling and Biochemical Properties

Marine Soulié, Anais Deletraz, Moheddine Wehbie, Florian Mahler, Benjamin Chantemargue, Ilham Bouchemal, Aline Le Roy, Isabelle Petit-Härtlein, Franck Fieschi, Cécile Breyton, Christine Ebel, Sandro Keller, and Grégory Durand*

Cite This: *ACS Appl. Mater. Interfaces* 2024, 16, 32971−32982 Read Online

ACCESS | Metrics & More | Article Recommendations | Supporting Information

ABSTRACT: We report herein the synthesis of three detergents bearing a perfluorinated cyclohexyl group connected through a short, hydrogenated spacer (i.e., propyl, butyl, or pentyl) to a β-maltoside polar head that are, respectively, called FCymal-3, FCymal-4, and FCymal-5. Increasing the length of the spacer decreased the critical micellar concentration (CMC), as demonstrated by surface tension (SFT) and isothermal titration calorimetry (ITC), from 5 mM for FCymal-3 to 0.7 mM for FCymal-5. The morphology of the micelles was studied by dynamic light scattering (DLS), analytical ultracentrifugation (AUC), and small-angle X-ray scattering (SAXS), indicating heterogeneous rod-like shapes. While micelles of FCymal-3 and -4 have similar hydrodynamic diameters of ∼10 nm, those of FCymal-5 were twice as large. We also investigated the ability of the detergents to solubilize lipid membranes made of 1-palmitoyl-2-oleyl-*sn*-glycero-3-phosphocholine (POPC). Molecular modeling indicated that the FCymal detergents generate disorder in lipid bilayers, with FCymal-3 being inserted more deeply into bilayers than FCymal-4 and -5. This was experimentally confirmed using POPC vesicles that were completely solubilized within 2 h with FCymal-3, whereas FCymal-5 required >8 h. A similar trend was noticed for the direct extraction of membrane proteins from *E. coli* membranes, with FCymal-3 being more potent than FCymal-5. An opposite trend was observed in terms of stabilization of the two model membrane proteins bacteriorhodopsin (bR) and SpNOX. In all three FCymal detergents, bR was stable for at least 2 months with no signs of aggregation. However, while the structural integrity of bR was fully preserved in FCymal-4 and -5, minor bleaching was observed in FCymal-3. Similarly, SpNOX exhibited the least activity in FCymal-3 and the highest activity in FCymal-5. By combining solubilizing and stabilizing potency, FCymal detergents push forward our expectations of the usefulness of fluorinated detergents for handling and investigating membrane proteins.

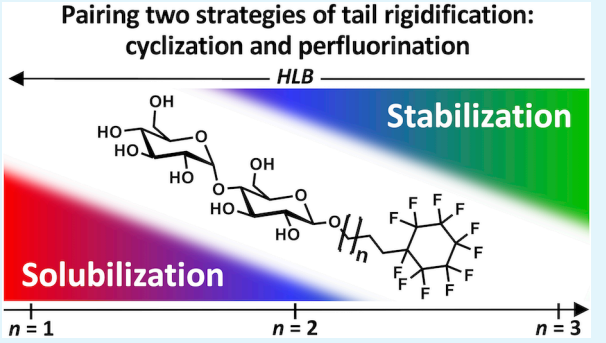

KEYWORDS: *detergents, micelles, membrane proteins, extraction, stabilization, rigidification, fluorine*

Downloaded via CEA SACLAY on July 4, 2024 at 12:17:47 (UTC).
See https://pubs.acs.org/sharingguidelines for options on how to legitimately share published articles.

INTRODUCTION

The growing interest in membrane proteins over the last decades is due to the fact that these proteins represent more than a quarter of all human proteins and constitute the largest class of drug targets.[1] However, studying membrane proteins remains a difficult challenge and requires a large panel of chemical tools: (i) to extract them from their native environment, (ii) to keep them soluble in aqueous solutions without denaturation or aggregation, and then (iii) to purify and characterize them in their functional states.

Several chemically engineered systems have been employed, but so far, none of them has been perfectly suited. From the simple "head-to-tail" detergents to more complex structures such as amphiphilic polymers, peptide-based amphiphiles, tripodal or facial detergents, increasing amount of efforts have been made over the two decades to enlarge the potential approaches to handle membrane proteins in solution.[2−4] Designing more sophisticated chemical tools is essential to addressing conflicting requirements in the handling of membrane proteins. Indeed, to extract membrane proteins from their native membrane, detergents have to provide efficient protein−detergent interactions to replace protein−lipid and protein−protein interactions but have to remain

Received: February 28, 2024
Revised: May 30, 2024
Accepted: May 31, 2024
Published: June 17, 2024

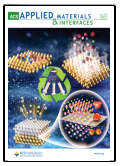

ACS Publications © 2024 American Chemical Society

sufficiently mild such that they do not destabilize membrane proteins by disrupting essential interactions or by delipidating them.

Over the past years, the conception of novel detergents for membrane protein studies has been focused on adjusting the hydrophilic−lipophilic balance,[5] the rigidity−flexibility balance,[6] and/or the shape.[7] Recent and notable works concentrate on the core foldability of the detergent to promote stabilizing properties;[8,9] unfortunately, however, extraction efficiency was not investigated thoroughly. Rigidification of alkyl chains is a promising way to obtain small, nondenaturing micelles. Such rigidification of the tail can be attained by substituting fluorine for hydrogen atoms, leading to fluorinated surfactants (FS, also called *F*-surfactants). *F*-surfactants are stabilizing toward fragile membrane proteins due to the bulkier and stiffer fluorinated alkyl chains,[6,10−12] but they can solubilize lipid membranes,[13] extract membrane proteins from membranes,[6,14−16] and promote the formation of protein−lipid nanodiscs.[17] Resorting to cyclic alkyl maltoside detergents is another promising strategy, as exemplified by the commercial Cymal series, where a β-maltoside polar head is linked to a hydrophobic tail made of a linear alkyl chain of *n* carbon atoms ended by a cyclohexyl group.[18] By introducing a cyclohexyl group to the tail, one can shorten the length of the alkyl chain of the detergent while keeping the same hydrophobicity. At the same time, the micelle size is significantly reduced, which can favor crystallization.[19−21] In addition to forming smaller protein/detergent complexes,[22] Cymal-6 and 7 have proven to maintain essential lipids around several secondary transporters, whereas Cymal-5 led to complete delipidation of these proteins.[23] As another example, PCC-Malt (4-trans-(4-trans-propylcyclohexyl)-cyclohexyl α-maltoside), with two alkyl cycles in the hydrophobic chain, efficiently extracts and stabilizes membrane proteins. In addition, it preserves the proper protein fold, improves thermostability and protein activity, and yields samples with promising quality for electron microscopy (EM).[24,25]

In this work, we present an original pairing between two strategies of rigidification of the hydrophobic domain of a detergent: perfluorination and cyclization. This is, to the best of our knowledge, the first example of cyclic perfluorinated detergents for the extraction and stabilization of membrane proteins. This will allow us to explore how modifying the rigidity of the hydrophobic domain and of the hydrophilic−lipophilic balance can alter both the extraction and the stabilization of membrane proteins. To this end, we report herein the synthesis of a series of three detergents bearing a perfluorinated cyclohexyl group connected through a short hydrogenated spacer (i.e., propyl, butyl, and pentyl) to a β-maltoside polar head; we call these detergents FCymal-3, FCymal-4, and FCymal-5, respectively (Figure 1).

Surface tension (SFT) and isothermal titration calorimetry (ITC) were used to evaluate the micellization properties of the detergents in water. Dynamic light scattering (DLS), analytical ultracentrifugation (AUC), and small-angle X-ray scattering (SAXS) were further used to investigate the size and shape of the micelles formed. Then, we monitored the interactions of the detergents with phospholipids by molecular dynamics (MD) simulations and the experimental solubilization of vesicle membranes made from 1-palmitoyl-2-oleyl-*sn*-glycero-3-phosphocholine (POPC), a singly unsaturated phospholipid. The extraction of membrane proteins contained in the *E. coli* membranes was investigated next. Finally, we evaluated the ability of these detergents to keep two model membrane proteins, bacteriorhodopsin (bR) and SpNOX, soluble, stable, and active.

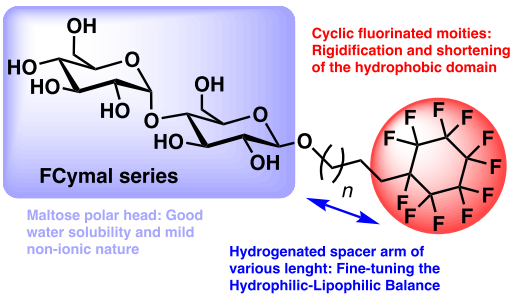

Figure 1. Chemical structures of cyclic fluorinated maltoside detergents (FCymals).

EXPERIMENTAL SECTION

Materials. Starting materials and solvents of reagent grade were commercially available and used as received. Anhydrous solvents were dried for 24 h of storage over activated 4-Å molecular sieves. Weakly acidic ion-exchange resin Amberlite CG-50 was used as obtained from Sigma−Aldrich to neutralize the pH of methanolic solution after deprotection of acetate groups under Zemplén conditions. Purifications were carried out on gravity silica gel column chromatography (pore size 60 Å, 230−400 mesh particle size, 40−63 μm particle size) or with a CombiFlash system. ^{1}H, ^{13}C, and ^{19}F NMR spectra were recorded on a Bruker AC400 spectrometer at 400, 100, and 375 MHz, respectively. Milli-Q water (resistivity of 18.2 MΩ cm and surface tension of 71.45 mN/m at 25 °C) was employed for all physicochemical experiments. Individual synthetic protocols as well as the complete chemical characterization of intermediary and final compounds are reported in the Supporting Information.

General Procedure for Glycosylation. Octa-O-acetyl-ß-D-maltose (1 equiv) was dissolved in dry CH_2Cl_2 (2 mL/mmol of sugar) under argon and stirred for 10 min at 0 °C. Allyl alcohol, 3-buten-1-ol or 4-penten-1-ol (1.6 equiv) was first added, followed by the dropwise addition of boron trifluoride diethyl ether complex (1.5 equiv). The mixture was stirred at 0 °C for 2 h and then kept at room temperature overnight. CH_2Cl_2 (20 mL) was added, and the crude mixture was washed with a saturated aqueous solution of $NaHCO_3$ (2 × 20 mL) and brine (2 × 20 mL). The organic layer was dried over Na_2SO_4 and evaporated under reduced pressure, and the crude product was purified by silica gel column chromatography using a mixture of cyclohexane/ethyl acetate as eluent.

General Procedure for Free Radical Addition. To a solution of **2a**, **2b**, or **2c** (1 equiv) in dry CH_2Cl_2 (10 mL/mmol) were added perfluorocyclohexyl iodide (1.4 equiv) and 1 M triethylborane in hexane (0.2 equiv). The mixture was flushed with air for 20 min and stirred at room temperature for 2 h. 50 mL of a diluted solution of $Na_2S_2O_3$ was added, and the aqueous solution was extracted with CH_2Cl_2 (2 × 50 mL). The organic fractions were collected, dried over anhydrous Na_2SO_4, and filtered, and the solvent was removed under reduced pressure. The crude compound was purified by silica gel column chromatography using a mixture of cyclohexane/ethyl acetate as eluent.

General Procedure for Iodinated Compound Reduction. To a solution of **3a**, **3b**, or **3c** (1.0 equiv) dissolved in methanol (15 mL/mmol), Pd/C (10% *w*/*w*) and sodium acetate (3.2 equiv) were added portion-wise, and the resulting solution was stirred overnight under $H_2(g)$ (6.5 bar). Then, the crude mixture was filtered over a pad of Celite, and the solvent was evaporated under reduced pressure. The crude compound was dissolved in CH_2Cl_2 (50 mL) and washed with a diluted solution of $Na_2S_2O_3$ (50 mL). Then the aqueous phase was extracted with CH_2Cl_2 (2 × 50 mL). The organic fractions were collected, dried over anhydrous Na_2SO_4, and filtered, and the solvent was removed under reduced pressure. The crude compound was

https://doi.org/10.1021/acsami.4c03359
ACS Appl. Mater. Interfaces 2024, 16, 32971−32982

purified by silica gel column chromatography using a mixture of cyclohexane/ethyl acetate as an eluent.

General Procedure of Deprotection under Zemplén Conditions. To a solution of **4a**, **4b**, or **4c** (1.0 equiv) in methanol was added a catalytic amount of sodium methoxide (0.4 equiv) portion-wise. The resulting solution was stirred at room temperature until total consumption of the reagent. The reaction mixture was neutralized by the addition of ion-exchange resin Amberlite CG-50 (2 g) and gentle stirring until pH = 6−7. The resin was filtered, and the solvent was evaporated under reduced pressure to afford the deprotected compound . The crude compound was purified by column chromatography on silica gel using a mixture of dichloromethane/methanol as eluent.

Hydrophile−Lipophile Balance Determination. HLB values were determined according to Griffin's method[26,27] using eq 1:

$$\mathrm{HLBG} = 20 \times \frac{M_h}{M} \quad (1)$$

where M is the molecular weight of the molecule and M_h is that of the hydrophilic part, here 342.3 g/mol.

HLB values were also determined according to Davies' method[28] using eq 3:

$$\mathrm{HLBD} = 7 + \sum \text{hydrophilic group numbers} + \sum \text{hydrophobic group numbers} \quad (2)$$

For the maltose group, a value of 1.9 for each primary −OH group (2 × 1.9) and a value of 0.5 for each secondary −OH groups (5 × 0.5) were assigned. We assigned 1.3 for each −O− (4 × 1.3). For the cyclic tail, the group numbers were −0.475 per each $-CH_2$ group and −0.870 per each $-CF_2$.[29] The first $-CH_2$ of the tail connected to maltose was excluded from the calculation[5,30] and the −CF− group connected to the CH_2 was counted like a CF_2.

Surface Tension Measurement (SFT). The surface activity of detergents at the air−water interface was determined using a K100 tensiometer (Kruss, Hamburg, Germany) in Milli-Q water. Surface tensions were measured using the Wilhelmy plate technique by dilution of stock solutions (13 g/L for FCymal-3, 4.6 g/L for FCymal-4, 2 g/L for FCymal-5, ∼4 × CMC). Stock solutions were equilibrated overnight before being diluted. In a typical experiment, 13 concentration steps were prepared and measured. All measurements were performed at (25.0 ± 0.5)°C until the standard deviation reached 0.05 mN/m or during at least 30 min.

Isothermal Titration Calorimetry (ITC). ITC experiments were performed at 25 °C using a VP-ITC instrument (Malvern Panalytics, Malvern, U.K.). Stock solutions of 45 mM for FCymal-3, 20 mM for FCymal-4, and 9 mM for FCymal-5 in phosphate buffer (10 mM NaH_2PO_4/Na_2HPO_4 and 150 mM NaCl at pH 7.4) were injected into the ITC sample cell containing only buffer. To allow complete re-equilibration after injection, the time spacing between two consecutive injections was chosen long enough. Baselines were subtracted from the experimental thermograms, followed by peak integration using NITPIC.[31] Further, demicellization isotherms were analyzed using D/STAIN giving the CMC, thermodynamic parameters, and corresponding 95% confidence intervals.[32]

Light Scattering (LS). LS measurements were carried out with a Nano Zetasizer S90 (Malvern, Herrenberg, Germany), utilizing a detection angle of 90° and a He−Ne laser at a wavelength of 633 nm as a light source. For DLS, solutions were transferred to a 45 μL quartz glass cuvette (Hellma, Munich, Germany) and equilibrated for 2 min before measurements. Attenuator settings were automatically set by the software. For static light scattering (SLS), the attenuator was fixed to the maximum position to ensure comparable results for light scattering intensities.

Sedimentation Velocity Experiments. Aqueous solutions of FCymal-3 between 6.1 and 12.6 mM, of FCymal-4 between 2 and 15 mM, and of FCymal-5 between 1 and 15 mM were prepared from 50 mM stock solutions. We used a Beckman XL-I analytical ultracentrifuge, a rotor Anti-50 (Beckman Coulter, Palo Alto, USA), and double-sector cells with optical path lengths of 0.15, 0.3, or 12 mm and Sapphire windows (Nanolytics, Potsdam, DE). Angular velocity 42,000 rpm (130 000 g), temperature 20 °C, and interference optics were used for data acquisition. Analysis in terms of continuous size distribution $c(s)$ of sedimentation coefficients, s, was done using SEDFIT v16.1c.[33] GUSSI v1.4.2[34] (http://biophysics.swmed.edu/MBR/software.html) was used for data manipulation. From the micelle signals at different concentrations, we derived the refractive index increment, $\partial n/\partial c$, and CMC using standard equations and protocols.[35] The CMC determined with ITC was, however, considered to derive from $s/s_0 = 1 - k'_s c$ (c is the micelle concentration in g/mL), s_0 the sedimentation coefficient extrapolated to zero concentration, and k'_s the hydrodynamic non-ideality factor. We used the Svedberg equation to estimate, at 5 mM above the CMC, from s and D_H—the hydrodynamic diameter from DLS—and using the detergent parameters reported in Table 2, the aggregation numbers, N_{agg}, and frictional coefficient, f/f_{min}.

SAXS Samples and Experiments. SAXS measurements were carried out in H_2O. Samples were prepared from stock samples at 50 mM using weighted solubilization and dilution. FCymal-3 was measured at 49.8, 25.5, 20.2, 15.4, 12.7, 9.8, 7.8, and 5.9 mM, FCymal-4 and FCymal-5 at 50, 25, 12.5, 6.25, 3.13 mM, and, additionally, 1.56 mM for the latter. SAXS acquisition was done on the BM29 beamline at the European Synchrotron Radiation Facility (Grenoble, France). Data were recorded in the range $0.004 < Q < 0.5$ Å^{-1} ($Q = (4\pi/\lambda)\sin\Theta$, 2Θ is the scattering angle, $\lambda = 0.9919$ Å is the wavelength), using a Pilatus3 2 M detector, at 20 °C, with a sample−detector distance of 2.867 m, for all samples except FCymal-3, where the detector was 1 M and the sample−detector distance was 2.864 m. Ten acquisitions of 1.0 s (0.5 s for FCymal-3) were recorded for 50 μL of the sample or the water solvent, loaded with a continuous flow in a quartz capillary. We used the automated standard beamline software (BSxCuBE)[36] for data reduction. Data processing was done using Primus/qT of the software suite ATSAS v2.8.4.[37] Absolute scales were obtained using the scattering of water (0.01632 cm^{-1} at 293 K).[36] The data of the session (MX1992 for FCymal-3 and MX/2189 for the other sets) are available on request. Details on the SAXS analysis are given in the Supporting Information.

Molecular Modeling. Each membrane, containing 128 lipid molecules, was created using the membrane bilayer builder from the CHARMM-GUI server.[38] The membranes were solvated with a hydration number of 40 water molecules per lipid. Na^+ and Cl^- ions were added at a 154 mM concentration. The force field parameters for the detergent molecules (DDM, F_6OM, FCymal-3, FCymal-4, and FCymal-5) were derived from the Generalized Amber Force Field 2 (GAFF2) using the Antechamber software.[39] Atomic charges were obtained using the restrained fit of electrostatic potential (RESP) based on the calculation performed at the HF/6-31G* level of theory using the R.E.D. III software.[40] The Slipids force field was used to describe lipid molecules, and the "three-point" TIP3P water model[41] was used to describe water molecules. Membrane property calculations are further detailed in the Supporting Information.

Preparation of Vesicles. POPC powder was weighed on an XP Delta Range microbalance (Mettler Toledo, Greifensee, Switzerland) and was suspended in buffer. The solution was vortexed at room temperature for 15 min and then extruded in a LiposoFast extruder (Avestin, Mannheim, Germany). In a typical preparation, at least 35 extrusion steps through two stacked polycarbonate membranes of 100 nm pore diameter (Avestin) were performed. The hydrodynamic diameter of the LUVs was monitored by DLS and found to be around 120−130 nm.

Kinetics of Vesicle Solubilization. The intensity of scattered light was recorded as a function of the time after mixing a high concentration of detergent (final concentration 5 mM above its CMC) and POPC LUVs (final lipid concentration 100 μM) in a 3 mm × 3 mm quartz glass cuvette.

Solubilization of Membrane Proteins from Native Membranes. *E. coli* BL21(DE3) cells transformed with an empty pET-24 vector were selected for kanamycin resistance, incubated in 400 mL of lysogenic broth (overnight, 37 °C, shaking at 150 rpm), harvested by

https://doi.org/10.1021/acsami.4c03359
ACS Appl. Mater. Interfaces 2024, 16, 32971−32982

Scheme 1. Synthesis of FCymal-3 (5a), FCymal-4 (5b), and FCymal-5 (5c)

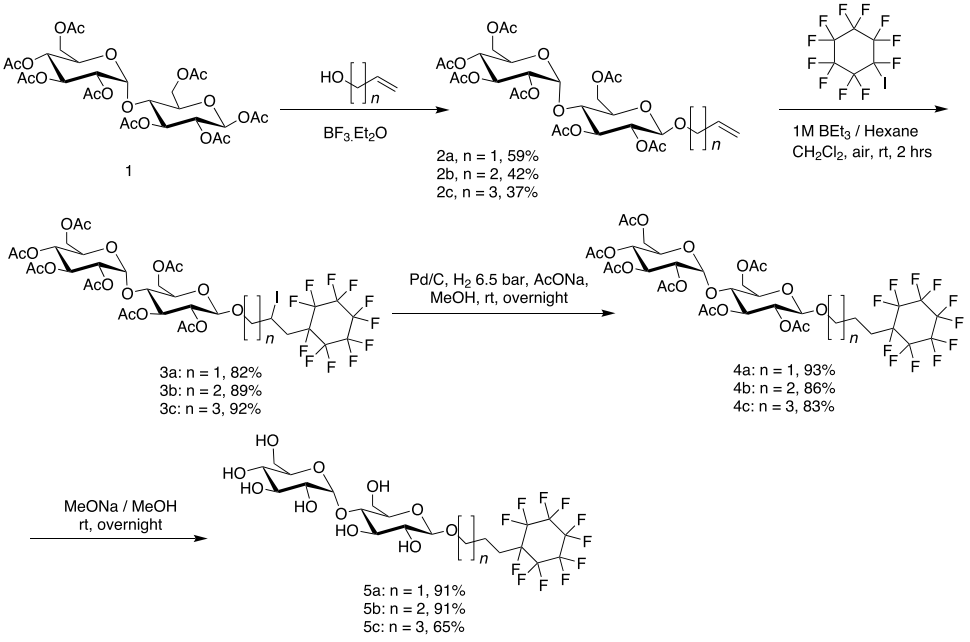

Table 1. Hydrophilic−Lipophilic Balance Calculated Based on the Griffin (HLBG) and Davies (HLBD) Methods and Micellization Properties of FCymal Detergents

detergent		FCymal-3	FCymal-4	FCymal-5
mol. weight (g/mol)		664	678	692
HLBG		10.3	10.1	9.9
HLBD		12.3	11.9	11.4
ITC[a]	CMC (mM)	5.06 ± 0.05	2.16 ± 0.03	0.69 ± 0.02
	$-T\Delta S^{\circ}_{mic}$ (kJ/mol)[b]	−28.6 ± 0.4	−30.4 ± 0.5	−32.4 ± 0.6
	ΔH°_{mic} (kJ/mol)[c]	5.5 ± 0.3	5.2 ± 0.5	4.4 ± 0.5
	ΔG°_{mic} (kJ/mol)[d]	−23.1 ± 0.0	−25.2 ± 0.0	−28.0 ± 0.1
	Δc_D	0.31 ± 0.04	0.16 ± 0.02	0.06 ± 0.02
SFT[a]	CMC (mM)	5.02 ± 0.00	2.29 ± 0.02	0.70 ± 0.01
	γ_{CMC} (mN/m)[e]	22.9 ± 2.1	22.7 ± 0.7	23.2 ± 0.2
	Γ_{max} (10^{-12} mol/mm^2)[f]	3.33 ± 0.15	3.51 ± 0.1	3.93 ± 0.1
	A_{min} (Å^2)[f]	49.6 ± 2.2	47.4 ± 1.1	42.3 ± 0.7
	ΔG_{mic} (kJ/mol)[d]	−23.1 ± 0.0	−25.0 ± 0.02	−27.9 ± 0.05

[a]Data are averages of at least two experiments. ± indicates standard errors from at least two experiments for SFT. [b]Entropic contribution to micelle formation. [c]Enthalpic contribution to micelle formation. [d]Gibbs energy of micellization. [e]Surface tension attained at the CMC. [f]Surface excess (Γ_{max}) and surface area per molecule (Å^2) were estimated from the slope of the surface tension curve.

centrifugation, and washed twice (154 mM NaCl saline). Resuspended cell pellets (ice-cold buffer, 100 mM Na_2CO_3, pH 11.5) were sonicated two times for 10 min each in an S-250A sonicator (Branson Ultrasonics, Danbury, USA). Cell debris was removed by centrifugation (4 °C, 20 min, 3000 *g*). Membrane fragments were separated from soluble and peripheral proteins by ultracentrifugation (4 °C, 1 h, 100,000 *g*). After washing, membrane pellets were resuspended in buffer and ultracentrifuged (4 °C, 1 h, 100,000 *g*). The resulting pellets were resuspended in buffer (50 mM Tris, 200 mM NaCl, pH 7.4) to yield a concentration of 100 mg of pellet wet weight per 1 mL of buffer. The CMC values measured in this study were used to adjust the detergent concentrations to ensure comparable extraction conditions. All samples were incubated (16 h, 20 °C, gentle shaking at 500 rpm) and ultracentrifuged (4 °C, 1 h, 100,000 *g*). The supernatant containing solubilized membrane proteins was analyzed by SDS−PAGE and FIJI for quantification.

bR Solubilization and Detergent Exchange Using Sucrose Gradient. We solubilized the purified purple membrane with bR at 1.5 g L^{-1}, for 40 h at 4 °C, using n-octyl-*β*-thioglucoside (OTG) at 89 mM (the CMC of the OTG is 9 mM) in 20 mM sodium phosphate buffer, pH 6.8 (bR buffer). We diluted the solubilized material to reach 15 mM for the final OTG concentration; we supplemented it with 2 mM of the tested detergent; and we incubated for 15 min. We then loaded the samples onto a 10−30% (*w*/*w*) sucrose gradient in bR buffer and CMC + 2 mM of either DDM as a control or of the tested detergent. We centrifuged the gradients at 55,000 rpm (200,000 *g*) for 5 h using a TLS55 rotor of a TL100 ultracentrifuge (Beckman). We easily recovered the BR-colored protein with a syringe. We kept the samples at 4 °C in the dark before monitoring them by UV−visible spectrophotometry.

SpNOX. SpNOX was overexpressed and purified according to reference[42] but in DDM and with 10 *μ*M FAD in all purification buffers. DDM was at 14.2 mM in the solubilization step, 14.2, 5.1, and 2.0 mM in the Ni-HisTrap column loading, washing, and elution steps. Size exclusion was done in 50 mM Tris-HCl pH 7.0, 300 mM NaCl, 10 *μ*M FAD, and 0.3 mM DDM. Activity assays were typically performed in triplicate after 10 times dilution of SpNOX at 0.15 mg/mL at the desired final detergent concentration and 2 h of incubation on ice. DDM concentration at this stage is estimated at 0.3 times the CMC, with the hypothesis of 1 g of DDM initially bound to 1 g

https://doi.org/10.1021/acsami.4c03359
ACS Appl. Mater. Interfaces 2024, 16, 32971−32982

SpNOX, in addition to buffer contribution. Activity assays were performed following Cytochrome c absorbance at 550 nm, after a further 5 times SpNOX dilution, in the presence of 100 μM cytochrome *c*, 10 μM FAD, and 200 μM NADPH. We measured specific activities of SpNOX in DDM at CMC + 2 mM, of 3.0 (±10%) mol Cyt *c* reduced s^{-1} mol^{-1} SpNOX, smaller but in line with reference.[43]

RESULTS AND DISCUSSION

Synthesis. The detergents were prepared according to a four-step synthetic route similar to that previously used for the synthesis of the linear fluorinated detergents F_5OM and F_5DM.[16] Compounds **2a**,[16] **2b**, and **2c**[16] were prepared by a glycosylation reaction between peracetylated maltose and allyl alcohol, buten-1-yl alcohol, or penten-1-yl alcohol, respectively, catalyzed by $BF_3.Et_2O$. The addition of the fluoroalkyl chain onto the double bond of compounds **2a**, **2b**, and **2c** was done by a free radical reaction with perfluorocyclohexyl iodide in the presence of 1 M BEt_3 in hexane. The iodine group of compounds **3a**, **3b**, and **3c** was removed under hydrogenolysis conditions in the presence of Pd/C as a catalyst. Finally, the desired detergents **5a**, **5b**, and **5c** were obtained by deprotection of compounds **4a**, **4b**, and **4c**, respectively, under Zemplén conditions, using a catalytic amount of MeONa in MeOH (Scheme 1). Purification of the crude detergents by silica gel chromatography followed by freeze-drying led to pure detergents with an overall yield of 20−40%.

Hydrophilic−Lipophilic Balance (HLB). The hydrophilic−lipophilic balance (HLB) allows one to classify common detergents and helps in their selection for handling membrane proteins.[5] The two common detergents DDM and OG are considered to be "mild" detergents toward membrane protein extraction and stabilization, their HLBG values being close to 12, a "well-balanced" value according to Breibeck and Rompel.[5] However, despite having similar HLBG values, DDM exhibits better stabilizing properties than OG, while OG exhibits higher extraction efficiencies. The HLB values of the FCymal derivatives were calculated according to the Griffin[26,27] (HLBG) and Davies[28] (HLBD) methods (Table 1). The Davies method takes into account the nature of the hydrophilic groups, i.e., stronger or weaker, as well as the contribution of the fluorinated carbons.[29,44] In contrast, the Griffin method is simply based on the ratio of the hydrophilic vs the total molar mass of the surfactant. Consequently, the Davies method yielded more pronounced differences in the HLB values among the FCymal detergents than the Griffin method, in agreement with our previous work on fluorinated glucose detergents.[30] Nevertheless, both methods unveiled the same trend within the FCymal series with longer spacer arms resulting in lower HLB values. Therefore, based on their HLB values between 10 and 12, the three FCymal detergents can be expected to exhibit a rather mild character toward membrane proteins. Moreover, FCymal-3 could exhibit solubilizing properties slightly better than those of FCymal-5, with the opposite behavior being expected for the stabilizing properties.

Micellization. Micellization of the three detergents in aqueous media was characterized by means of ITC and SFT (Figures 2 and S1), from which we derived micellar parameters (Table 1).

ITC showed that the CMC values decreased with increasing *n*, from 5.06 mM for FCymal-3 to 0.69 mM for FCymal-5; the CMC of FCymal-4 was found in between at 2.16 mM. SFT showed the same trend with CMC values in very good agreement with those from ITC. Thus, the addition of two methylene groups to the chain led to a decrease in the CMC by about 1 order of magnitude, as expected on the basis of Traube's rule.[45] This decrease in the CMC with increasing chain length was primarily driven by a more favorable change in entropy, with the enthalpy making only a minor contribution.

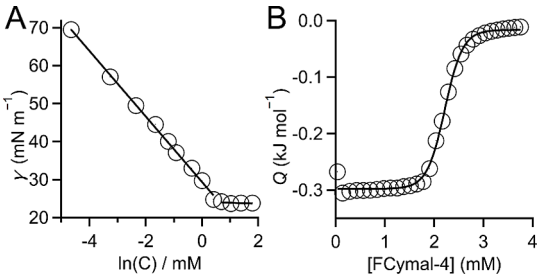

Figure 2. (A) Surface tension vs concentration for FCymal-4 in Milli-Q water. The solid line is a linear fit of the experimental data (open symbols), and the intersection corresponds to the CMC. (B) ITC data for FCymal-4 in phosphate buffer. The solid line is a fit to the experimental isotherm (open symbols) based on a generic sigmoidal function.

The surface tension at the CMC, γ_{CMC}, was found to be around 23 mN/m for all three detergents, which is slightly higher than that of linear fluorinated maltosides.[16] SFT data were used to construct Gibbs adsorption isotherms (Figures 2 and S1) to determine the surface excess concentration at surface saturation, Γ_{max}, and the area occupied per detergent molecule at the air/water interface, A_{min}. The values observed for the FCymal detergents were similar for the three compounds. Γ_{max} slightly varied from 3.33×10^{-12} mol/mm^2 for FCymal-3 to 3.93×10^{-12} mol/mm^2 for FCymal-5, thus indicating somewhat tighter packing when the length of the hydrogenated spacer was increased. An opposite trend was observed for the occupied areas, which ranged from 49.9 Å^2 for FCymal-3 to 42.3 Å^2 for FCymal-5. By contrast, linear fluorinated maltosides exhibit occupied areas of ∼60 Å^2, indicating that the three cyclic fluorinated detergents introduced here pack more tightly at the air/water interface.

Micelle Size and Shape. The self-assembly properties of the fluorinated detergents were investigated in pure water by using DLS, AUC, and SAXS (Table 2). At 10 × CMC, volume-weighted particle size distributions revealed unimodal distributions of micelles with hydrodynamic diameters ranging from ∼12 nm for FCymal-3 and FCymal-4 to ∼22 nm for FCymal-5 (Figure 3). By comparison, the two linear fluorinated maltosides F_5OM and F_5DM showed a unimodal distribution with diameters of 8 and 15 nm, respectively.[16]

Intensity-weighed particle size distributions (Figure S2) revealed multimodal distributions for the three detergents. However, the main fraction was always found in small assemblies with hydrodynamic diameters ranging from ∼20 nm for FCymal-3 and FCymal-4 to ∼46 nm for FCymal-5, with larger aggregates of 300−1000 nm in diameter accounting for only a small fraction of the total material present in the samples (Figure S2). By varying the detergent concentration from 6 to 16 × CMC, a slight increase in the diameter was observed both in volume-weighted (Figure 3) and in intensity-weighted distributions (data not shown).

The size distributions of three detergent assemblies were further investigated by sedimentation velocity AUC. The *c*(*s*)

https://doi.org/10.1021/acsami.4c03359
ACS Appl. Mater. Interfaces 2024, 16, 32971−32982

Table 2. DLS, AUC, and SAXS Data of FCymal Detergents

		FCymal-3	FCymal-4	FCymal-5
	M (Da)[a]	664.4	678.4	692.5
	$\bar{\nu}$ (mL/g)[a]	0.564	0.576	0.587
	$\partial\rho_{el}/\partial c$ (cm g^{-1})[a]	3.38×10^{10}	3.28×10^{10}	3.19×10^{10}
DLS	d (nm) − Int.[b]	20.2 ± 0.3	18.9 ± 0.4	45.9 ± 2.2
	d (nm) − Vol.[b]	12.6 ± 0.2	12.5 ± 0.4	21.7 ± 0.8
	d_0 (nm) − Vol[b]	9	10	21
AUC	s_0 (S)[c]	7.7	9.3	26.2
	s (S)[d]	9.8	11.1	29.5
	N_{agg}[d]	198	250	2615
	f/f_{min}[d]	1.67	1.69	2.98
SAXS	R_g (nm)[e]	5.7 ± 0.1	10.0 ± 0.0	14.3 ± 0.0
	N_{agg}[e]	78	404	1060
	D_{max} (nm)[e]	29 ± 3	50 ± 5	120 ± 5
	R_c (nm)[e]	1.4	1.5	1.8
	R (nm)	1.5	1.6	2.1
	L (nm)	14	27	115

[a]Molar mass and partial specific volume calculated from the chemical composition. [b]Hydrodynamic diameters by dynamic light scattering measured in water at 10 × CMC for FCymal-3 (49.6 mM), FCymal-4 (21.5 mM), and FCymal-5 (8.05 mM) and calculated at infinite dilution (d_0). Data are averages of at least three measurements made of ten runs. [c]Sedimentation coefficient at infinite dilution. [d]Sedimentation coefficient interpolated at CMC + 5 mM (10.1, 7.2, and 5.7 mM for FCymal-3, FCymal-4, and FCymal-5, respectively). Aggregation numbers and frictional ratios obtained from s and d at CMC + 5 mM. Error is estimated at 10%. [e]Results at 15.4, 12.5, and 8.05 mM for FCymal-3, FCymal-4, and FCymal-5, respectively. Radius of gyration (R_g) and aggregation number (N_{agg}) from Guinier analysis, maximum intramolecular distances (D_{max}) from $P(r)$ analysis, cross-sectional radius of gyration (R_c) from ln $I(Q)Q$ vs Q^2 analysis, radius (R) and length (L) from analysis as cylinders with a fixed polydispersity index of 0.35 for R and L. For FCymal-5, flexibility improved the fit, the resulting Kuhn segment length is 30 nm.

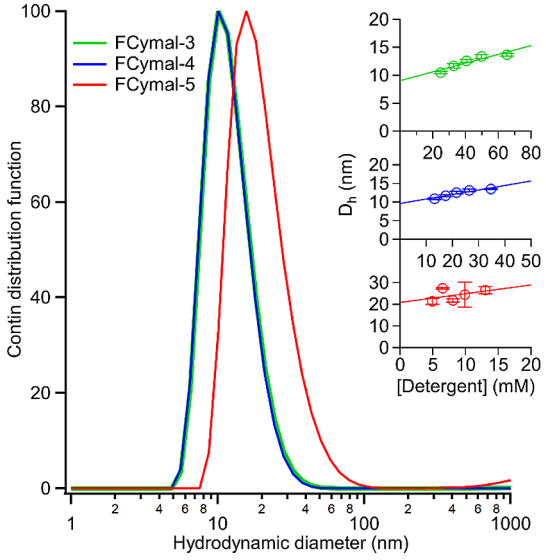

Figure 3. Volume-weighted particle size distributions of FCymal-3, FCymal-4, and FCymal-5 at 49.6, 21.5, and 8.05 mM in water, corresponding to micellar concentrations of 45, 19, and 7.7 mM, respectively. The inset shows the dependence of the hydrodynamic diameters on the concentrations for the three detergents.

distributions displayed a slow sedimenting species at ≈ ∼1 S, representing the monomers, and a larger distribution corresponding to the micelles which appear to be always heterogeneous (Figure 4A). Micelles of FCymal-4 appeared

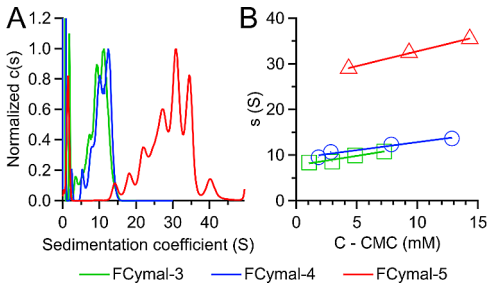

Figure 4. (A) Normalized $c(s)$ of FCymal-3, FCymal-4, and FCymal-5 at 9.9, 5.0, and 5.0 mM (corresponding to micellar concentrations of 4.9, 2.8, and 4.3 mM, respectively). (B). Mean micelle s-values vs micelle concentration up to 15 mM for FCymal-3, FCymal-4, and FCymal-5 (green squares, blue circles, and red triangles, respectively).

slightly larger than those of FCymal-3, while micelles of FCymal-5 were much larger. For the three detergents, the micelle size increased with detergent concentration (Figure S3). The mean s-values for the micelles increased linearly with the detergent concentration (Figure 4B), allowing extrapolation of the sedimentation coefficient to infinite dilution, s_0. Other parameters derived from the $c(s)$ integration are given in Table S1. Combining the interpolated s and d from DLS, we derived mean aggregation numbers, N_{agg}, and frictional ratios f/f_{min} (Table 2). N_{agg} increased with the length of the hydrogenated spacer between the polar head and the cyclohexyl group, with values of 200, 250, and 2600 for FCymal-3, FCymal-4, and FCymal-5, respectively. The larger f/f_{min} values for the larger aggregation numbers suggest an increased shape anisotropy of the detergent micelles. A positive correlation between micelle sizes and thermodynamic stability for a large number of membrane proteins has been reported.[46] Detergents with a short chain form compact micelles of small size and destabilize membrane proteins more than detergents with a longer chain. Fluorinated surfactants with polar headgroup of various sizes also showed a correlation between micelle sizes and membrane protein stability.[47] Therefore, based on the size of the micelles formed by the FCymal derivatives, one can expect FCymal-5 to be more stabilizing than FCymal-3.

The solution structure of the cyclic fluorinated detergents was further characterized using SAXS. Figure 5A−C presents the superposition of the concentration-normalized scattering curves, the Guinier plots, and $P(r)$ analysis for micellar concentrations of ∼10 mM. The propensity to form large aggregates was correlated to the length of the hydrogenated spacer with radii of gyration, R_g, close to 6 nm for FCymal-3, 10 nm for FCymal-4, and 14 nm for FCymal-5. Derived aggregation numbers (N_{agg} ≈ 80, 400, 1100, respectively) and maximum intramolecular distances (D_{max} ≈ 30, 50, 120 nm, respectively) changed accordingly (Table 2). At the intermediate angular range, the (ln $I(Q)Q$ vs Q^2) representation shows straight lines, suggesting that the detergents form rod-shaped micelles (Figure S4A), with cross-sectional radii of gyration, R_c, ranging from 1.4 to 1.8 nm. All three detergents showed a propensity to form large aggregates at higher concentrations, as seen in the analysis in terms of R_g, N_{agg}, and D_{max} values at various detergent concentrations, with R_c remaining constant above 10 mM (Figure S5, Tables S2−

https://doi.org/10.1021/acsami.4c03359
ACS Appl. Mater. Interfaces 2024, 16, 32971−32982

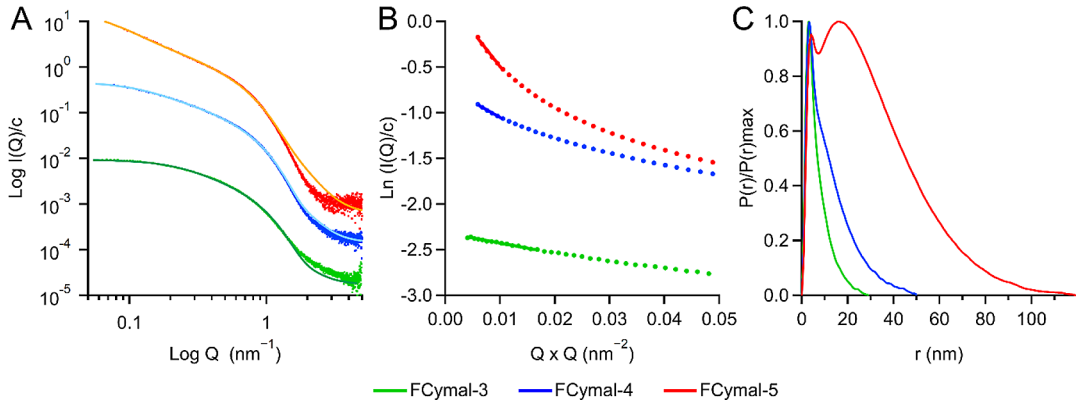

Figure 5. SAXS analysis of FCymal-3, FCymal-4, and FCymal-5 at 15.4, 12.5, and 8.05 mM, respectively, which corresponds to a micellar concentration of ∼10 mM. Scattering intensities, I, are in absolute scale. Q is the scattering vector (nm^{-1}). (A) Normalized scattering curves and fitted curves considering a cylinder shape, in light green, cyan, and orange, for FCymal-3, FCymal-4, and FCymal-5, respectively. For clarity, data for FCymal-3 and FCymal-5 are displayed shifted by +1 and −1 Log units, respectively. (B) Guinier plots, with the linear extrapolation used for R_g and $I(0)$ determination (continuous lines). (C) $P(r)$, the pair distribution function, vs r, the intramolecular distances (nm).

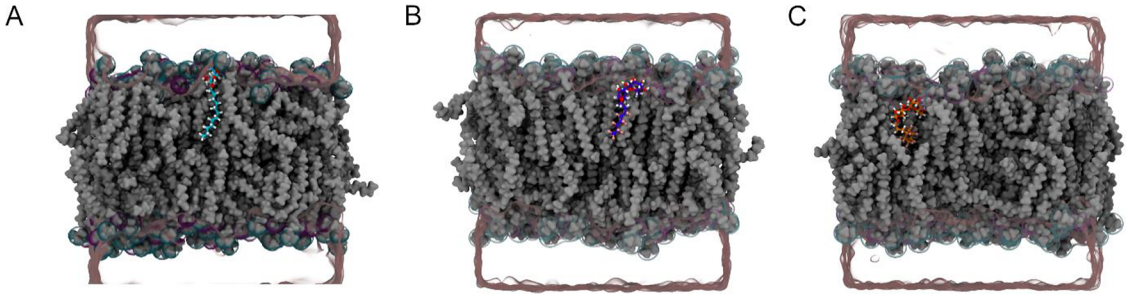

Figure 6. Average position and orientation of the detergent molecules, depicted in cyan, purple, and orange for DDM (A), F_6OM (B), and FCymal-3 (C), respectively.

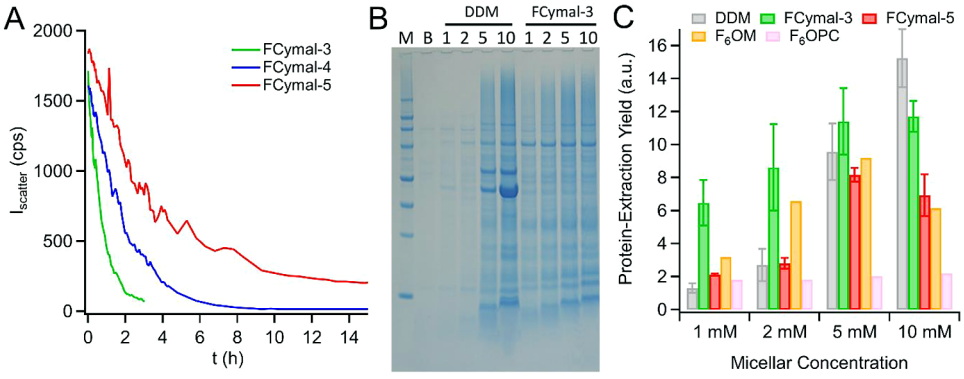

Figure 7. (A) Vesicle solubilization kinetics. 0.3 mM POPC LUVs solubilized by CMC + 5 mM FCymal-3 (10.06 mM), FCymal-4 (7.16 mM), and FCymal-5 (5.69 mM) at 50 °C as monitored as the light scattering intensity recorded at an angle of 90°. (B) SDS−PAGE of *E. coli* membrane extracts upon exposure to various DDM or FCymal-3 concentrations. Values indicate detergent concentrations in units of millimolar above the respective CMC. (C) Yields of protein extraction for the new and established detergents. The yields are given as relative values after the subtraction of the background value when no detergent was added. Data are means from three replicates, and error bars indicate standard deviations.

S4). We analyzed the whole scattering curves considering a cylindrical shape using the software SASview (Figures 5A and S4B, Tables 2 and S5). Flexibility improved the fit for the FCymal-5, with a resulting Kuhn segment length of 30 nm, but not for FCymal-3 and FCymal-4. The fitted lengths of the cylinder increased with the length of the hydrogenated spacer, with values of 14, 27, and 115 m for FCymal-3, FCymal-4, and FCymal-5, respectively. By contrast, the fitted radii increased only moderately, with values of 1.5, 1.6, and 2.1 nm for FCymal-3, FCymal-4, and FCymal-5, respectively. These values are in line with those of R_g, N_{agg}, and R_c (Table 2).

Molecular Modeling. To investigate the interactions of the fluorinated detergents with lipid membranes, we carried out MD simulations using bilayers made from POPC, a singly unsaturated zwitterionic phospholipid. Each membrane, containing 128 POPC molecules, was solvated with 40 water molecules per lipid in the presence of Na^+ and Cl^- ions at 154 mM. The POPC bilayer was equilibrated for 500 ns before detergent molecules were successively placed at two different

https://doi.org/10.1021/acsami.4c03359
ACS Appl. Mater. Interfaces 2024, 16, 32971−32982

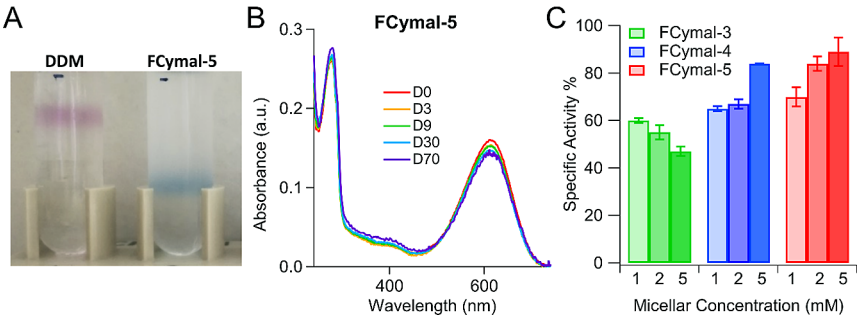

Figure 8. (A) Sucrose gradients (10−30%) of bR in the presence of FCymal-4 and FCymal at 5 CMC + 2 mM, in 20 mM Na_2PO_4 pH 6.8 buffer, after centrifugation at 200,000 *g* for 5 h. (B) Spectral time course of bR transferred by sucrose gradient centrifugation in FCymal-5 at CMC + 2 mM. UV−visible spectra of bR incubated at 4 °C in the dark were recorded at different times (indicated in days (D)), with time 0 for the sample freshly recovered from the gradient. (C) Specific Activity of SpNOX in detergents at various micellar concentrations: light corresponds to CMC + 1 mM, medium to CMC + 2 mM and dark to CMC + 5 mM. The specific activity was normalized to that measured in DDM at CMC + 2 mM.

positions: (i) at the water−membrane interface or (ii) preinserted into the lipid bilayer. For the sake of comparison, DDM, one of the most widely used detergents, and F_6OM its commercially available perfluorinated analogue were included as well. For each simulation, 8 detergent molecules per leaflet were included in the membrane model (corresponding to 12.5% mol, simulating a high concentration of detergents). Structural analyses were performed over the last 800 ns (except for FCymal-3 inserted at the water−membrane interface simulation, for which the last 400 ns were used) for each simulation to ensure enough sampling over well-equilibrated systems.

We first studied the positioning and orientation of the detergent molecules within the POPC bilayer. We observed that the sugar headgroups of the detergents are located between the phosphate and the glycerol moieties of POPC (Figures 6 and S6, Table S6). A slightly deeper insertion, based on the acyl chain oxygen position, was noted for both F_6OM and FCymal-3 when compared with DDM. In contrast, FCymal-4 and FCymal-5 were inserted at a depth similar to that of DDM (Figure S6).

The orientations of both DDM and F_6OM were found to be perpendicular to the membrane surface and aligned almost parallel to the acyl chains of POPC (Figure 6A,B). By contrast, the three cyclic detergents introduced herein exhibited more tilted orientations, with that of FCymal-3 being the most pronounced (Figure 6C). The bulkiness of the fluorinated cycle might be the reason for the tilted orientation (Figure 7). The liquid−disordered phase of the lipids could also push the molecules toward a more tilted orientation. It is worth noting that, when the detergent molecules were inserted at the water−membrane interface, DDM formed small aggregates at the interface with the sugar moieties toward the water and the hydrogenated chains toward the interior of the aggregate (Figure S8), as opposed to the fluorinated detergents, which inserted rapidly into the membrane without forming any aggregates.

We next examined the impact of the detergents on the POPC bilayer. The area per lipid, A_l, was significantly affected by the presence of the four fluorinated detergents and DDM at the sugar moieties located between the phosphate and glycerol moieties of POPC (Table S6), thus perturbing the packing of the polar heads (Table S7). This is characteristic of a disordering effect on the polar heads and supported by an increase in K_A, the area compressibility modulus (see Supporting Information), indicating more tension at the polar heads. However, a decrease in electrostatic repulsion and an increase in hydrogen bonding from the glycerol moiety were also noted (Table S7). Finally, we observed a slightly deeper insertion of F_6OM compared with the other fluorinated molecules.

Membrane insertion of the detergents tends to reduce the number of water molecules around the glycerol moieties of POPC, as shown in Figure S9. The bulky sugar moieties tend to form more hydrogen bonds with the surrounding glycerol moieties of the lipids, thus preventing water molecules from penetrating more deeply below the polar head region. The disordering effect of the fluorinated detergents was observed for both the saturated acyl chain and the end of the unsaturated chain of POPC (Figures S10 and S11). This can be explained by the location of the fluorinated cycle above the double bond of the unsaturated chain. In conclusion, the bulkiness and lipophobic nature of the fluorinated cycle together with the tilted orientation of the detergent molecules lead to lipid disordering.

Vesicles Solubilization and Membrane Protein Extraction. To investigate the ability of the FCymal series to solubilize lipid bilayers, we monitored the solubilization of large unilamellar vesicles (LUVs) made of POPC using light scattering measurements. At 25 °C, the addition of a rather high concentration (CMC + 5 mM) of the cyclic fluorinated detergents to LUVs at a lipid concentration of 0.3 mM resulted in a monotonic decrease in the light scattering intensity over time, demonstrating that all three compounds were able to dissolve preformed membranes, albeit with different kinetics (Figure 7A). While FCymal-3 led to complete and rapid solubilization of the membranes within 2 h, FCymal-5 required a significantly longer incubation time of >8 h, with FCymal-4 being in between. Thus, we observed a trend between the length of the hydrogenated spacer and the kinetics of solubilization, with longer chains resulting in slower solubilization. This demonstrates that modulation of the spacer's length has a profound impact on the ability of the cyclic fluorinated detergents to interact with lipid bilayers, as suggested by molecular modeling. The potency of the three compounds to solubilize POPC vesicles at 25 °C sets them apart from more conventional fluorinated surfactants such as F_6OM and fluorinated DigluM compounds, which require elevated temperatures and prolonged incubation times for solubilization.[14]

Next, we investigated whether the cyclic fluorinated detergents could also extract membrane proteins from native

https://doi.org/10.1021/acsami.4c03359
ACS Appl. Mater. Interfaces 2024, 16, 32971−32982

E. coli membranes. The intensities of the SDS−PAGE band patterns were quantified by pixel counts for FCymal-3 (Figure 7B) and FCymal-5 (not shown) and were compared with those of DDM, F_6OM, and F_6OPC (Figure 7C). Then, overall protein-extraction yields were expressed relative to buffer without any detergent. Figure 7B shows that FCymal-3 efficiently extracted a broad size range of membrane proteins from *E. coli* membranes. At low concentrations (i.e., CMC + 1−5 mM), FCymal-3 displayed even better solubilization efficiencies than DDM. Both FCymal-5 and F_6OM extracted less but still significant amounts of membrane proteins, with maximum yields being obtained at detergent concentrations equal to the CMC + 5 mM in both cases. The superior detergency of FCymal-3 over FCymal-5 correlates with the HLB values (Table 1). In stark contrast with these findings, the fluorinated nondetergent F_6OPC did not extract significantly more proteins than what was present in the buffer-only negative control. Generally, the extraction efficiency of detergents increases with their concentration,[18] as observed here for DDM. Interestingly, the three fluorinated detergents introduced here do not follow this trend, as they reach maximum extraction efficiency at CMC + 5 mM.

Stability and Enzymatic Activity of Membrane Proteins. Last, we investigated the ability of the detergents to keep two model membrane proteins soluble and in their native form. We first used bacteriorhodopsin (bR). By binding a retinal molecule as a covalent cofactor, bR's visible absorption spectrum is an excellent reporter of its structural integrity, with the λ_{max} of the retinal molecule being very sensitive to its local environment. The native state of the bR protein can be easily evaluated and, thus, the stabilizing properties of detergents.[47] Figure 8A shows sucrose density gradients obtained with DDM and FCymal-5. The sharp colored bands indicate the formation of homogeneous protein−detergent complexes under all conditions, and the lower position of bR when in fluorinated detergents reflects a denser protein/surfactant complex, both in full agreement with previous observations.[47] A variation in color was also noted: when solubilized in detergent, the monomeric protein was characterized by λ_{max} = 554 nm, and the protein appeared purple/pink as in DDM. When transferred into a fluorinated detergent, λ_{max} shifts to 615 nm, giving a blue color to the protein−surfactant complex, as we have already reported.[47] When transferred into the cyclic fluorinated detergents, the same shift was observed (Figures 8B and S12). Importantly, in all three FCymal detergents, bR was stable over the 2 month period tested, with no signs of aggregation observed. In addition, no changes in the absorption spectrum, neither in value nor in intensity, were observed for FCymal-4 and FCymal-5 (Figures 8B and S12), attesting to the excellent structural stability of bR in these detergents. In FCymal-3, a minor loss in the intensity of the retinal absorption peak without a concomitant increase in the peak at 380 nm suggested some bleaching of bR (Figure S12). When comparing the structural and colloidal stabilities of bR in the different fluorinated maltosides investigated so far,[16,48,49] it is clear that these cyclic fluorinated detergents are the most promising ones.

Moreover, we studied the enzymatic stability of SpNOX from *Streptococcus pneumonia*, a protein that is analogous to eukaryotic NADPH oxidase.[42] Enzymatic activities measured after detergent exchange are displayed in Figure 8C. In FCymal-3, SpNOX exhibited moderate activity compared with DDM over the range of concentrations tested (47−60%). The activity was higher for FCymal-4 (65−84%) and FCymal-5 (70−89%). It is hard to ascertain the relevance of the slight variation in activity with detergent concentration in the investigated range. Nonetheless, the stabilizing properties of the cyclic detergents toward SpNox are better than those of linear fluorinated maltosides, for which only 30−50% of the maximum activity was measured.[16] Our results highlight the ability of the cyclic fluorinated detergents to stabilize bR and SpNOX in active forms. Moreover, this stabilizing activity seems to be correlated with the length of the hydrogenated spacer between the polar head and the perfluorinated cyclohexyl group, with FCymal-5 and FCymal-4 being more stabilizing than FCymal-3. Although the biochemical evaluation of the FCymal derivatives was conducted on a limited number of systems, namely, two model membranes and two rather stable membrane proteins, in agreement with previous observations,[5,46] we observe that increasing the length of the tail and, thus, decreasing the HLB of the detergent results in larger micelles that provide a more stabilizing environment. By contrast, decreasing the length of the tail and, thus, increasing the HLB lead to the formation of smaller micelles with improved detergency but lower stabilizing properties.

CONCLUSIONS

We have designed a series of head-and-tail detergents whose tail is made of a perfluorinated cyclohexyl moiety attached to a maltose polar head through a short, hydrogenated spacer of three to five carbon atoms. The synthesis of the compounds is straightforward, leading in four steps to pure detergents with a 20−40% overall yield. Thus, further optimization and scaling-up of the synthesis could allow the broad dissemination of these compounds. The three FCymal detergents were found to have well-defined CMCs whose values linearly decrease with the length of the hydrogenated spacer from 5.0 to 0.7 mM, in full agreement with the behavior of conventional head-and-tail detergents. By contrast, the length of the spacer does not affect the physicochemical properties of the detergents at the air/water interface. With regard to the size and shape of the micelles, we observed rather heterogeneous aggregates with a hydrodynamic diameter ranging from 9 to 21 nm and with a radius of gyration ranging from 5 to 15 nm within the series. Our data suggest the formation of rod-like micelles, with those of FCymal-3 and FCymal-4 having similar sizes, whereas those of Cymal-5 are significantly longer but with a similar diameter. Molecular modeling revealed disordering effects of the three FCymal detergents on POPC bilayers, while complete solubilization of POPC vesicles was experimentally observed in a few hours by the three FCymal detergents, with the shortest hydrogenated spacer resulting in the fastest solubilization. The detergency was also demonstrated with *E. coli* membranes, from which a broad range of membrane proteins were extracted; again, the extraction efficiency was found to increase with a decrease in the length of the spacer. Of note, linear fluorinated detergents have previously failed to show significant extraction. This suggests that the simultaneous presence of a short, hydrogenated spacer and a bulky perfluorinated cyclohexyl moiety is responsible for the detergency. Finally, we demonstrated that the FCymal detergents were able to keep the two membrane proteins bR and SpNox stable and active after extraction using classical detergents and exchange of the detergent into the FCymal detergents. The stabilizing properties of the FCymal detergents

https://doi.org/10.1021/acsami.4c03359
ACS Appl. Mater. Interfaces 2024, 16, 32971−32982

were anticorrelated with their lipid-solubilization and protein-extraction efficiencies. Specifically, the longest spacer of FCymal-5 conferred the most potent stabilizing properties toward both bR and SpNox, outperforming previously tested fluorinated detergents. By combining solubilizing and stabilizing potency, this series of FCymal detergents pushes forward our expectations on the usefulness of fluorinated detergents for handling and investigating membrane proteins.

■ ASSOCIATED CONTENT

Supporting Information

The Supporting Information is available free of charge at https://pubs.acs.org/doi/10.1021/acsami.4c03359.

Detailed synthetic protocols; SAXS analysis; calculation of membrane properties; SFT and ITC data of FCymal-3 and FCymal-5; intensity-weighted particle size distributions in water by DLS; superposition of $c(s)$ of FCymal detergents at various concentrations; analysis of SAXS scattering curves in terms of rods; analysis of FCymal SAXS data in term of R_g, N_{agg}, D_{max}, and R_c; electron density profiles; representation of different orientation of FCymal in POPC bilayer; representation of aggregation of DDM in water/POPC bilayer interface; quantification and representation of hydration of glycerol moieties of lipids in the presence of FCymal; order parameter of POPC atoms in presence or absence of detergents; impact of detergents on the lipid's position in the bilayer; time denaturation of bR by UV−vis spectroscopy in the presence of FCymal; parameters derived from AUC analysis; structural analysis by SAXS using Primus/qT of FCymal-3, FCymal-4, and FCymal-5; details of the analysis of SAXS data in terms of cylinder; z-position of the center of mass (COM) of the different lipid and detergent molecules; and parameters of the POPC bilayer with and without detergent (PDF)

■ AUTHOR INFORMATION

Corresponding Author

Grégory Durand − *Institut des Biomolécules Max Mousseron (UMR 5247 UM-CNRS-ENSCM), Equipe Chimie Bioorganique et Systèmes amphiphiles, 84916 Avignon Cedex 9, France; Avignon Université, Unité Propre de Recherche et d'Innovation, Equipe Synthèse et Systèmes Colloïdaux Bio-organiques, 84916 Avignon Cedex 9, France;* orcid.org/0000-0001-6680-2821; Phone: +33 490144445; Email: gregory.durand@univ-avignon.fr

Authors

Marine Soulié − *Institut des Biomolécules Max Mousseron (UMR 5247 UM-CNRS-ENSCM), Equipe Chimie Bioorganique et Systèmes amphiphiles, 84916 Avignon Cedex 9, France; Avignon Université, Unité Propre de Recherche et d'Innovation, Equipe Synthèse et Systèmes Colloïdaux Bio-organiques, 84916 Avignon Cedex 9, France*

Anais Deletraz − *Institut des Biomolécules Max Mousseron (UMR 5247 UM-CNRS-ENSCM), Equipe Chimie Bioorganique et Systèmes amphiphiles, 84916 Avignon Cedex 9, France*

Moheddine Wehbie − *Institut des Biomolécules Max Mousseron (UMR 5247 UM-CNRS-ENSCM), Equipe Chimie Bioorganique et Systèmes amphiphiles, 84916 Avignon Cedex 9, France*

Florian Mahler − *Molecular Biophysics, Technische Universität Kaiserslautern (TUK), 67663 Kaiserslautern, Germany*

Benjamin Chantemargue − *InSiliBio, Limoges 87069, France*

Ilham Bouchemal − *Univ. Grenoble Alpes, CNRS, CEA, CNRS, IBS, F-38000 Grenoble, France*

Aline Le Roy − *Univ. Grenoble Alpes, CNRS, CEA, CNRS, IBS, F-38000 Grenoble, France*

Isabelle Petit-Härtlein − *Univ. Grenoble Alpes, CNRS, CEA, CNRS, IBS, F-38000 Grenoble, France*

Franck Fieschi − *Univ. Grenoble Alpes, CNRS, CEA, CNRS, IBS, F-38000 Grenoble, France; Institut Universitaire de France (IUF), 75005 Paris, France;* orcid.org/0000-0003-1194-8107

Cécile Breyton − *Univ. Grenoble Alpes, CNRS, CEA, CNRS, IBS, F-38000 Grenoble, France;* orcid.org/0000-0002-4382-0434

Christine Ebel − *Univ. Grenoble Alpes, CNRS, CEA, CNRS, IBS, F-38000 Grenoble, France*

Sandro Keller − *Biophysics, Institute of Molecular Biosciences (IMB), NAWI Graz, University of Graz, 8010 Graz, Austria; Field of Excellence BioHealth, University of Graz, 8010 Graz, Austria; BioTechMed-Graz, 8010 Graz, Austria;* orcid.org/0000-0001-5469-8772

Complete contact information is available at: https://pubs.acs.org/10.1021/acsami.4c03359

Notes

The authors declare the following competing financial interest(s): Moheddine Wehbie and Gregory Durand are co-inventors of a patent that covers the cyclic fluorinated detergents presented in this study.

■ ACKNOWLEDGMENTS

This work was funded by the Agence Nationale de la Recherche (ANR-16-CE92-0001), by the Deutsche Forschungsgemeinschaft (DFG, grant no. KE 1478/7 1), and by the Austrian Science Fund (FWF, grant no. I 5359-N). We acknowledge the financial support of the European Regional Development Fund, the French Government, the "Région Provence Alpes Côte d'Azur", the "Département de Vaucluse" and the "Communauté d'agglomération Grand Avignon" for access to the NMR platform (CPER 3A). This work used the platforms of the Grenoble Instruct-ERIC center (ISBG; UAR 3518 CNRS-CEA-UGA-EMBL) within the Grenoble Partnership for Structural Biology (PSB), supported by FRISBI (ANR-10-INBS-0005-02) and GRAL, financed within the University Grenoble Alpes graduate school (Ecoles Universitaires de Recherche) CBH-EUR-GS (ANR-17-EURE-0003). IBS acknowledges integration into the Interdisciplinary Research Institute of Grenoble (IRIG, CEA). We acknowledge the European Synchrotron Radiation Facility for provision of synchrotron radiation facilities, and we would like to thank Marc Tully for assistance in using beamline BM29. This work benefited from the use of the SasView application, originally developed under NSF Award DMR - 0520547. SasView also contains code developed with funding from the EU Horizon 2020 program under the SINE2020 project Grant No 654000. We thank Emmi Mikkola (UGA) who participated in the

biochemical evaluation. We thank Dr Pierre Guillet (AU) for assistance in the preparation of the figures.

REFERENCES

(1) Yin, H.; Flynn, A. D. Drugging Membrane Protein Interactions. *Annu. Rev. Biomed. Eng.* **2016**, *18*, 51−76.
(2) Ratkeviciute, G.; Cooper, B. F.; Knowles, T. J. Methods for the solubilisation of membrane proteins: the micelle-aneous world of membrane protein solubilisation. *Biochem. Soc. Trans.* **2021**, *49* (4), 1763−1777.
(3) Thoma, J.; Burmann, B. M. Fake It 'Till You Make It—The Pursuit of Suitable Membrane Mimetics for Membrane Protein Biophysics. *International Journal of Molecular Sciences* **2021**, *22* (1), 50.
(4) Zhang, Q.; Cherezov, V. Chemical tools for membrane protein structural biology. *Curr. Opin. Struct. Biol.* **2019**, *58*, 278−285.
(5) Breibeck, J.; Rompel, A. Successful amphiphiles as the key to crystallization of membrane proteins: Bridging theory and practice. *Biochimica et Biophysica Acta (BBA) - General Subjects* **2019**, *1863* (2), 437−455.
(6) Durand, G.; Abla, M.; Ebel, C.; Breyton, C., *New Amphiphiles to Handle Membrane Proteins: "Ménage à Trois" Between Chemistry, Physical Chemistry, and Biochemistry*. In Membrane Proteins Production for Structural Analysis, Mus-Veteau, I., Ed. Springer: New York, 2014; pp 205−251.
(7) Urner, L. H.; Ariamajd, A.; Weikum, A. Combinatorial synthesis enables scalable designer detergents for membrane protein studies. *Chemical Science* **2022**, *13* (35), 10299−10307.
(8) Ghani, L.; Kim, S.; Wang, H.; Lee, H. S.; Mortensen, J. S.; Katsube, S.; Du, Y.; Sadaf, A.; Ahmed, W.; Byrne, B.; Guan, L.; Loland, C. J.; Kobilka, B. K.; Im, W.; Chae, P. S. Foldable Detergents for Membrane Protein Study: Importance of Detergent Core Flexibility in Protein Stabilization. *Chemistry* **2022**, *28* (21), No. e202200116.
(9) Das, M.; Mahler, F.; Hariharan, P.; Wang, H.; Du, Y.; Mortensen, J. S.; Patallo, E. P.; Ghani, L.; Glück, D.; Lee, H. J.; Byrne, B.; Loland, C. J.; Guan, L.; Kobilka, B. K.; Keller, S.; Chae, P. S. Diastereomeric Cyclopentane-Based Maltosides (CPMs) as Tools for Membrane Protein Study. *J. Am. Chem. Soc.* **2020**, *142* (51), 21382−21392.
(10) Hashimoto, M.; Murai, Y.; Morita, K.; Kikukawa, T.; Takagi, T.; Takahashi, H.; Yokoyama, Y.; Amii, H.; Sonoyama, M. Comparison of functionality and structural stability of bacteriorhodopsin reconstituted in partially fluorinated dimyristoylphosphatidylcholine liposomes with different perfluoroalkyl chain lengths. *Biochimica et Biophysica Acta (BBA) - Biomembranes* **2021**, *1863* (10), 183686.
(11) Baba, T.; Takagi, T.; Sumaru, K.; Kanamori, T. Effect of the fluorination degree of partially fluorinated octyl-phosphocholine surfactants on their interfacial properties and interactions with purple membrane as a membrane protein model. *Chem. Phys. Lipids* **2020**, *227*, 104870.
(12) Popot, J.-L. Amphipols, nanodiscs, and fluorinated surfactants: three nonconventional approaches to studying membrane proteins in aqueous solutions. *Annu. Rev. Biochem.* **2010**, *79*, 737−775.
(13) Frotscher, E.; Danielczak, B.; Vargas, C.; Meister, A.; Durand, G.; Keller, S. A Fluorinated Detergent for Membrane-Protein Applications. *Angew. Chem., Int. Ed.* **2015**, *54* (17), 5069−5073.
(14) Boussambe, G. N. M.; Guillet, P.; Mahler, F.; Marconnet, A.; Vargas, C.; Cornut, D.; Soulie, M.; Ebel, C.; Le Roy, A.; Jawhari, A.; Bonnete, F.; Keller, S.; Durand, G. Fluorinated diglucose detergents for membrane-protein extraction. *Methods* **2018**, *147*, 84−94.
(15) Soulié, M.; Deletraz, A.; Wehbie, M.; Mahler, F.; Bouchemal, I.; Le Roy, A.; Petit-Härtlein, I.; Keller, S.; Meister, A.; Pebay-Peyroula, E.; Breyton, C.; Ebel, C.; Durand, G. Zwitterionic fluorinated detergents: From design to membrane protein applications. *Biochimie* **2023**, *205*, 40−52.
(16) Wehbie, M.; Onyia, K. K.; Mahler, F.; Le Roy, A.; Deletraz, A.; Bouchemal, I.; Vargas, C.; Babalola, J. O.; Breyton, C.; Ebel, C.; Keller, S.; Durand, G. Maltose-Based Fluorinated Surfactants for Membrane-Protein Extraction and Stabilization. *Langmuir* **2021**, *37* (6), 2111−2122.
(17) Mahler, F.; Meister, A.; Vargas, C.; Durand, G.; Keller, S. Self-Assembly of Protein-Containing Lipid-Bilayer Nanodiscs from Small-Molecule Amphiphiles. *Small* **2021**, *17* (49), No. 2103603.
(18) Arachea, B. T.; Sun, Z.; Potente, N.; Malik, R.; Isailovic, D.; Viola, R. E. Detergent selection for enhanced extraction of membrane proteins. *Protein Expression Purif.* **2012**, *86* (1), 12−20.
(19) Ostermeier, C.; Harrenga, A.; Ermler, U.; Michel, H. Structure at 2.7 Å resolution of the Paracoccus denitrificans two-subunit cytochrome c oxidase complexed with an antibody FV fragment. *Proc. Natl. Acad. Sci. U. S. A.* **1997**, *94* (20), 10547−10553.
(20) Guan, R. J.; Xiang, Y.; Wang, M.; Li, G. P.; Wang, D. C. Crystallization and preliminary X-ray analysis of a depressant insect toxin from the scorpion Buthus martensii Karsch. *Acta Crystallogr., Sect. D: Biol. Crystallogr.* **2001**, *57* (Pt 9), 1313.
(21) Nukaga, M.; Abe, T.; Venkatesan, A. M.; Mansour, T. S.; Bonomo, R. A.; Knox, J. R. Inhibition of class A and class C beta-lactamases by penems: crystallographic structures of a novel 1,4-thiazepine intermediate. *Biochemistry* **2003**, *42* (45), 13152−9.
(22) Kunji, E. R. S.; Harding, M.; Butler, P. J. G.; Akamine, P. Determination of the molecular mass and dimensions of membrane proteins by size exclusion chromatography. *Methods* **2008**, *46* (2), 62−72.
(23) Ilgü, H.; Jeckelmann, J. M.; Gachet, M. S.; Boggavarapu, R.; Ucurum, Z.; Gertsch, J.; Fotiadis, D. Variation of the detergent-binding capacity and phospholipid content of membrane proteins when purified in different detergents. *Biophys. J.* **2014**, *106* (8), 1660−70.
(24) Missel, J. W.; Salustros, N.; Becares, E. R.; Steffen, J. H.; Laursen, A. G.; Garcia, A. S.; Garcia-Alai, M. M.; Kolar, Č.; Gourdon, P.; Gotfryd, K. Cyclohexyl-α maltoside as a highly efficient tool for membrane protein studies. *Current research in structural biology* **2021**, *3*, 85−94.
(25) Hovers, J.; Potschies, M.; Polidori, A.; Pucci, B.; Raynal, S.; Bonneté, F.; Serrano-Vega, M. J.; Tate, C. G.; Picot, D.; Pierre, Y.; Popot, J.-L.; Nehmé, R.; Bidet, M.; Mus-Veteau, I.; Bußkamp, H.; Jung, K.-H.; Marx, A.; Timmins, P. A.; Welte, W. A class of mild surfactants that keep integral membrane proteins water-soluble for functional studies and crystallization. *Molecular Membrane Biology* **2011**, *28* (3), 171−181.
(26) Griffin, W. C. Calculation of HLB Values of Non-Ionic Surfactants. *J. Soc. Cosmet. Chem.* **1954**, *5*, 249−256.
(27) Griffin, W. C. Classification of Surface-Active Agents by "HLB. *J. Soc. Cosmet. Chem.* **1949**, *1*, 311−326.
(28) Davies, J. T. A quantitative kinetic theory of emulsion type, I. Physical chemistry of the emulsifying agent. *Proc. Int. Congr. Surf. Act., 2nd* **1957**, 426−438.
(29) Lin, I. J. Hydrophile-lipophile balance (hlb) of fluorocarbon surfactants and its relation to the critical micelle concentration (cmc). *J. Phys. Chem.* **1972**, *76* (14), 2019−2023.
(30) Wehbie, M.; Bouchemal, I.; Deletraz, A.; Pebay-Peyroula, E.; Breyton, C.; Ebel, C.; Durand, G. Glucose-Based Fluorinated Surfactants as Additives for the Crystallization of Membrane Proteins: Synthesis and Preliminary Physical−Chemical and Biochemical Characterization. *ACS Omega* **2021**, *6* (38), 24397−24406.
(31) Keller, S.; Vargas, C.; Zhao, H.; Piszczek, G.; Brautigam, C. A.; Schuck, P. High-Precision Isothermal Titration Calorimetry with Automated Peak-Shape Analysis. *Anal. Chem.* **2012**, *84* (11), 5066−5073.
(32) Tso, S.-C.; Mahler, F.; Höring, J.; Keller, S.; Brautigam, C. A. Fast and Robust Quantification of Detergent Micellization Thermodynamics from Isothermal Titration Calorimetry. *Anal. Chem.* **2020**, *92* (1), 1154−1161.
(33) Schuck, P. Size-distribution analysis of macromolecules by sedimentation velocity ultracentrifugation and lamm equation modeling. *Biophys. J.* **2000**, *78* (3), 1606−19.

https://doi.org/10.1021/acsami.4c03359
ACS Appl. Mater. Interfaces 2024, 16, 32971−32982

(34) Brautigam, C. A., *Chapter Five - Calculations and Publication-Quality Illustrations for Analytical Ultracentrifugation Data*. In Methods in Enzymology, Cole, J. L., Ed. Academic Press: 2015; Vol. *562*, pp 109−133.
(35) Salvay, A. G.; Ebel, C. *Analytical Ultracentrifuge for the Characterization of Detergent in Solution*. In Analytical Ultracentrifugation VIII, Wandrey, C.; Cölfen, H., Eds. Springer: Berlin, Heidelberg, 2006; Vol. *131*.
(36) Orthaber, D.; Bergmann, A.; Glatter, O. SAXS experiments on absolute scale with Kratky systems using water as a secondary standard. *J. Appl. Crystallogr.* **2000**, *33* (2), 218−225.
(37) Franke, D.; Petoukhov, M. V.; Konarev, P. V.; Panjkovich, A.; Tuukkanen, A.; Mertens, H. D. T.; Kikhney, A. G.; Hajizadeh, N. R.; Franklin, J. M.; Jeffries, C. M.; Svergun, D. I. ATSAS 2.8: a comprehensive data analysis suite for small-angle scattering from macromolecular solutions. *J. Appl. Crystallogr.* **2017**, *50* (4), 1212−1225.
(38) Wu, E. L.; Cheng, X.; Jo, S.; Rui, H.; Song, K. C.; Dávila-Contreras, E. M.; Qi, Y.; Lee, J.; Monje-Galvan, V.; Venable, R. M.; Klauda, J. B.; Im, W. CHARMM-GUI Membrane Builder toward realistic biological membrane simulations. *Journal of computational chemistry* **2014**, *35* (27), 1997−2004.
(39) Wang, J.; Wolf, R. M.; Caldwell, J. W.; Kollman, P. A.; Case, D. A. Development and testing of a general amber force field. *Journal of computational chemistry* **2004**, *25* (9), 1157−74.
(40) Dupradeau, F.-Y.; Pigache, A.; Zaffran, T.; Savineau, C.; Lelong, R.; Grivel, N.; Lelong, D.; Rosanski, W.; Cieplak, P.; The, R. E. D. Tools: advances in RESP and ESP charge derivation and force field library building. *Phys. Chem. Chem. Phys.* **2010**, *12* (28), 7821−7839.
(41) Jämbeck, J. P. M.; Lyubartsev, A. P. Another Piece of the Membrane Puzzle: Extending Slipids Further. *J. Chem. Theory Comput.* **2013**, *9* (1), 774−784.
(42) Hajjar, C.; Cherrier, M. V.; Dias Mirandela, G.; Petit-Hartlein, I.; Stasia, M. J.; Fontecilla-Camps, J. C.; Fieschi, F.; Dupuy, J. The NOX Family of Proteins Is Also Present in Bacteria. *mBio* **2017**, *8* (6), No. e01487-17.
(43) Breyton, C.; Javed, W.; Vermot, A.; Arnaud, C.-A.; Hajjar, C.; Dupuy, J.; Petit-Hartlein, I.; Le Roy, A.; Martel, A.; Thépaut, M.; Orelle, C.; Jault, J.-M.; Fieschi, F.; Porcar, L.; Ebel, C. Assemblies of lauryl maltose neopentyl glycol (LMNG) and LMNG-solubilized membrane proteins. *Biochimica et Biophysica Acta (BBA) -. Biomembranes* **2019**, *1861* (5), 939−957.
(44) Lin, I. J.; Marszall, L. CMC, HLB, and effective chain length of surface-active anionic and cationic substances containing oxyethylene groups. *J. Colloid Interface Sci.* **1976**, *57* (1), 85−93.
(45) Tanford, C. Thermodynamics of micelle formation: prediction of micelle size and size distribution. *Proc. Natl. Acad. Sci. U. S. A.* **1974**, *71* (5), 1811−5.
(46) Kotov, V.; Bartels, K.; Veith, K.; Josts, I.; Subhramanyam, U. K. T.; Günther, C.; Labahn, J.; Marlovits, T. C.; Moraes, I.; Tidow, H.; Löw, C.; Garcia-Alai, M. M. High-throughput stability screening for detergent-solubilized membrane proteins. *Sci. Rep.* **2019**, *9* (1), 10379.
(47) Breyton, C.; Gabel, F.; Abla, M.; Pierre, Y.; Lebaupain, F.; Durand, G.; Popot, J.-L.; Ebel, C.; Pucci, B. Micellar and Biochemical Properties of (Hemi)Fluorinated Surfactants Are Controlled by the Size of the Polar Head. *Biophys. J.* **2009**, *97* (4), 1077−1086.
(48) Polidori, A.; Raynal, S.; Barret, L.-A.; Dahani, M.; Barrot-Ivolot, C.; Jungas, C.; Frotscher, E.; Keller, S.; Ebel, C.; Breyton, C.; Bonnete, F. Sparingly fluorinated maltoside-based surfactants for membrane-protein stabilization. *New J. Chem.* **2016**, *40* (6), 5364−5378.
(49) Polidori, A.; Presset, M.; Lebaupain, F.; Ameduri, B.; Popot, J.-L.; Breyton, C.; Pucci, B. Fluorinated and hemifluorinated surfactants derived from maltose: Synthesis and application to handling membrane proteins in aqueous solution. *Bioorg. Med. Chem. Lett.* **2006**, *16* (22), 5827−5831.

NOTE ADDED AFTER ASAP PUBLICATION

This paper originally published ASAP on June 17, 2024. Due to a production error, several graphics were not correct. The corrected version of this paper was reposted on June 18, 2024.

https://doi.org/10.1021/acsami.4c03359
ACS Appl. Mater. Interfaces 2024, 16, 32971−32982